Near-infrared multi-wavelengths long persistent luminescence of Nd3+ ion through persistent energy transfer in Ce3+, Cr3+ co-doped Y3Al2Ga3O12 for the first and second bio-imaging windows

Jian Xu, Setsuhisa Tanabe, Atul D. Sontakke, and Jumpei Ueda

Citation: Applied Physics Letters **107**, 081903 (2015); doi: 10.1063/1.4929495
View online: http://dx.doi.org/10.1063/1.4929495
View Table of Contents: http://scitation.aip.org/content/aip/journal/apl/107/8?ver=pdfcov
Published by the AIP Publishing

APPLIED PHYSICS LETTERS **107**, 081903 (2015)

Near-infrared multi-wavelengths long persistent luminescence of Nd^{3+} ion through persistent energy transfer in Ce^{3+}, Cr^{3+} co-doped $Y_3Al_2Ga_3O_{12}$ for the first and second bio-imaging windows

Jian Xu, Setsuhisa Tanabe,[a] Atul D. Sontakke, and Jumpei Ueda
Graduate School of Human and Environmental Studies, Kyoto University, Kyoto 606-8501, Japan

(Received 10 June 2015; accepted 8 August 2015; published online 24 August 2015)

We developed a persistent phosphor of $Y_3Al_2Ga_3O_{12}$ doped with Nd^{3+}, Ce^{3+}, Cr^{3+} ions (YAGG:Nd-Ce-Cr) exhibiting long (>10 h) persistent luminescence at multi-wavelengths of around 880, 1064, and 1335 nm due to f-f transitions of Nd^{3+} and at 505 nm due to Ce^{3+}:$5d_1 \rightarrow 4f$ transition. The intense near-infrared (NIR) persistent luminescence bands from Nd^{3+} match well with the first (650–950 nm) and second (1000–1400 nm) bio-imaging windows. The NIR persistent radiance of the YAGG:Nd-Ce-Cr phosphor (0.33×10^{-1} mW/Sr/m^2) at 60 min after ceasing blue light illumination was over 2 times higher than that of the widely used $ZnGa_2O_4$:Cr^{3+} red persistent phosphor (0.15×10^{-1} mW/Sr/m^2). © *2015 AIP Publishing LLC*.
[http://dx.doi.org/10.1063/1.4929495]

Recently, persistent phosphors (sometimes named as long-lasting phosphors) have attracted much attention for *in vivo* bio-imaging applications since these nano-particle phosphors charged by ultraviolet (UV) light (visible light in rare cases) before injection into biological tissues can emit red and/or near-infrared (NIR) persistent luminescence lasting for minutes to even several hours without further real-time illumination.[1–4] The exclusion of external illumination removes the possibility of autofluorescence as background noise and thus improves the signal-to-noise ratio remarkably. This application motivates the considerable development of the red/NIR persistent phosphors with bright radiance and long afterglow.[5–8] However, only a few red/NIR long persistent phosphors have been reported so far, most of which are Cr^{3+} doped gallate- or aluminate-based materials,[9–14] and their emission regions are mostly located in the first bio-imaging window (NIR-I window, 650–950 nm).

Combined with fast development and availability of InGaAs detectors, the second bio-imaging window (NIR-II window, 1000–1400 nm) has promising advantages owing to its lower autofluorescence, deeper tissue penetration, and thus potentially higher spatial and temporal resolution than the NIR-I window.[15] Till now, although several types of optical probes for the NIR-II window have been developed such as single-walled carbon nanotubes[16] and semiconductor quantum dots composed of highly toxic heavy metals,[17] the development of nontoxic and biocompatible luminescent materials emitting in the NIR region, especially in the NIR-II window, still remains a challenge. Although persistent phosphors can be promising candidates for bio-imaging, only few of them are suitable for the NIR-II window and their persistent durations are quite short (only up to few minutes),[18–20] which limits their practical applications.

Recently, a garnet persistent phosphor of Ce^{3+}, Cr^{3+} co-doped $Y_3Al_{5-x}Ga_xO_{12}$ (YAGG:Ce-Cr) has been developed by our group.[21–24] In this material, Cr^{3+} acts as an electron trap with ideal trap depth at $x = 3$ for persistent luminescence of Ce^{3+} working at room temperature (RT). Based on our previous work, we developed a persistent phosphor of $Y_3Al_2Ga_3O_{12}$:Nd^{3+}, Ce^{3+}, Cr^{3+} (YAGG:Nd-Ce-Cr). This material can be excited by blue light (460 nm) and emit green persistent luminescence due to Ce^{3+}: $5d_1 \rightarrow 4f$ for over 10 h. Furthermore, thanks to the highly efficient energy transfer (ET) from Ce^{3+} to Nd^{3+} in garnet hosts,[25–27] it can also show NIR persistent luminescence for almost the same duration due to Nd^{3+}: $^4F_{3/2} \rightarrow {}^4I_{9/2}$, $^4I_{11/2}$, $^4I_{13/2}$ transitions, matching well with the NIR-I and NIR-II windows. A persistent phosphor with such a wide emission range (green to NIR) and long (>10 h) persistent duration has never been reported before and we thus state as a discovery.

YAGG:Nd-Ce-Cr and YAGG:Nd ceramic phosphors with the composition of $Y_{2.955}Ce_{0.015}Nd_{0.03}Al_{1.999}Cr_{0.001}Ga_3O_{12}$ and $Y_{2.97}Nd_{0.03}Al_2Ga_3O_{12}$, respectively, were fabricated by a solid-state reaction method. Y_2O_3 (99.99%), Al_2O_3 (99.99%), Ga_2O_3 (99.99%), CeO_2 (99.99%), Nd_2O_3 (99.99%), and Cr_2O_3 (99.9%) were used as raw materials. The starting powder was mixed by ball milling method with anhydrous alcohol for several hours. The mixed powder was dried at 80 °C for 36 h, compacted to form a ceramic green body (ϕ20 mm, 2 mm thickness) under uniaxial pressing of 50 MPa, and finally sintered at 1600 °C for 24 h in air. The YAGG:Ce-Cr ($Y_{2.985}Ce_{0.015}Al_{1.999}Cr_{0.001}Ga_3O_{12}$) ceramic phosphor prepared by the same experimental procedure was used as a reference sample.[22]

The diffuse reflectance spectra of the ceramic samples were measured by a spectrophotometer (UV3600, Shimadzu) equipped with an integrating sphere. Photoluminescence (PL) spectra of the YAGG:Ce-Cr and YAGG:Nd-Ce-Cr samples were recorded in the range of 400–1600 nm by pumping with a 442 nm laser diode (NDHB510APA-E, Nichia Co. Ltd.,) excitation. The PL spectra were measured by a monochromator (G250, Nikon), a Si photodiode (PD) detector (S-025-H, Electro-Optical System Inc.) from 400 to 800 nm and an InGaAs PD detector (IGA-030-H, Electro-Optical

[a]E-mail: tanabe.setsuhisa.4v@kyoto-u.ac.jp

System Inc.) from 800 to 1600 nm. All the PL spectra were calibrated by using a standard halogen lamp (SCL-600, Labsphere). Persistent luminescence (PersL) spectra of the two samples were measured by a Si CCD spectrometer (QE65-Pro, Ocean Optics) from 400 to 1000 nm and an InGaAs CCD spectrometer (NIR 512, Ocean Optics) from 1000 to 1600 nm connected with an optical fiber. All the PersL spectra were calibrated using the same halogen lamp. A 300 W Xe lamp (MAX-302, Asahi Spectra) with UV mirror module (250–400 nm) was used as the excitation source for thermoluminescence (TL) measurements. The ceramic sample was set in a cryostat (Helitran LT3, Advanced Research Systems) to control temperatures and first illuminated by the UV light at 150 K for 10 min, then heated up to 550 K at a rate of 10 K/min at 10 min after ceasing the illumination, and the TL signals were recorded by the Si PD (spectral sensitivity covers from 300 to 1200 nm). The Si CCD spectrometer was operated simultaneously with the TL measurement to always monitor the TL spectra at different temperatures. All persistent luminescent decay curves of the samples after being excited for 5 min by the Xe lamp with a 460 nm band-pass filter were measured at 25 °C using the Si PD. In order to monitor the Ce^{3+} emission, the Si PD was covered with a short-cut filter (<475 nm) and a long-cut filter (>650 nm) to filter out all but the Ce^{3+} luminescence. Then the decay curves were calibrated to the absolute luminance (in unit of mcd/m^2) using a radiance meter (Glacier X, B&W Tek Inc.). In order to monitor the Nd^{3+} luminescence, the Si PD was covered with an 800 nm short-cut filter to filter out all but the Nd^{3+} luminescence. Then the decay curves were calibrated to the absolute radiance (in unit of mW/Sr/m^2) using the same radiance meter. Photographs of the samples were taken by a digital camera (EOS kiss X5, Canon), and the settings remained constant: exposure time–5 s, ISO value–1600, and aperture value (F value)–5.0.

Fig. 1(a) shows the PL spectra of the YAGG:Ce-Cr and YAGG:Nd-Ce-Cr samples under blue laser (442 nm) excitation. The YAGG:Ce-Cr sample exhibits an intense emission band centered at 505 nm, corresponding to the f-d transition from the lowest 5d energy level ($5d_1$) to the 4f ground state of Ce^{3+}. Besides, a weak emission band at around 690 nm is ascribed to the $^2E \rightarrow {}^4A_2$ transition (*R*-line) of Cr^{3+}. Comparing the PL spectrum of the YAGG:Ce-Cr sample with the diffuse reflectance of the Nd^{3+} singly doped YAGG sample (YAGG:Nd), the absorption bands ($^4I_{9/2} \rightarrow {}^2G_{3/2}$, $^4G_{7/2}$, $^2G_{7/2}$, $^4G_{5/2}$) of Nd^{3+} are overlapped with the emission range of Ce^{3+} indicating that the ET process from Ce^{3+} to Nd^{3+} can efficiently occur. This is confirmed by the decrease of Ce^{3+} emission intensity in the visible range and the presence of several sharp emission bands at around 880 nm, 1064 nm, and 1335 nm owing to the f-f transitions of Nd^{3+}: $^4F_{3/2} \rightarrow {}^4I_{9/2}$, $^4I_{11/2}$, and $^4I_{13/2}$, respectively, in the YAGG:Nd-Ce-Cr sample.

The PersL spectra of the YAGG:Nd-Ce-Cr sample recorded at different times after ceasing blue illumination are shown in Fig. 1(b). The persistent emission bands exhibit not only a broad band located at around 500 nm due to Ce^{3+}: $5d_1 \rightarrow 4f$ transition but also intense sharp bands located at the NIR region (around 880 nm, 1064 nm, and 1335 nm) due to the f-f transitions of Nd^{3+}, which match well with the NIR-I and NIR-II windows. The identical shape of its PL and PersL spectra suggests that the emission centers are the same under and after excitation. Since the ET process from Ce^{3+} to Nd^{3+} occurs in PL, we assume that the similar energy transfer process called persistent energy transfer (persistent ET) also occurs in the YAGG:Nd-Ce-Cr phosphor after ceasing the excitation source. The phenomenon of the persistent ET has been confirmed previously in $CaAl_2O_4$:Tb^{3+}, Ce^{3+} (Refs. 28 and 29) and $Sr_4Al_{14}O_{25}$:Cr^{3+}, Eu^{2+}, Dy^{3+} (Ref. 30) persistent phosphors.

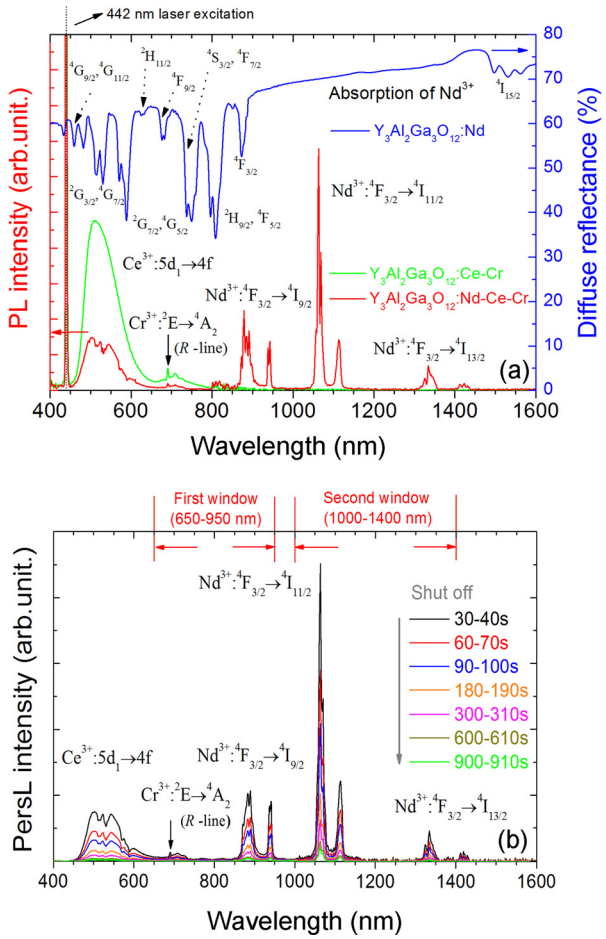

FIG. 1. (a) PL spectra of the YAGG:Ce-Cr and YAGG:Nd-Ce-Cr ceramics as well as the diffuse reflectance of the YAGG:Nd ceramic and (b) PersL spectra of the YAGG:Ce-Cr and YAGG:Nd-Ce-Cr ceramics (integrating time: 10 s).

The persistent luminescent decay curve monitoring Ce^{3+} emission (475–650 nm) of the YAGG:Nd-Ce-Cr sample after ceasing blue light illumination is shown in Fig. 2(a), in which the decay curves of the standard YAGG:Ce-Cr ceramic phosphor and a compacted ceramic pellet made of the well-known $SrAl_2O_4$:Eu^{2+}-Dy^{3+} (SAO:Eu-Dy) commercial phosphor (LumiNova- GLL300FFS, Nemoto & Co. Ltd.) under the same experimental condition are also plotted as references.[22] The luminance values at 60 min after ceasing the excitation are 11 mcd/m^2 for YAGG: Nd-Ce-Cr, 30 mcd/m^2 for YAGG:Ce-Cr, and 25 mcd/m^2 for SAO:Eu-Dy, respectively (see the photographs of the two ceramics under and after blue LED illumination in Fig. 2(d)). Persistent luminescence durations to reach a luminance of 0.32 mcd/m^2 in the YAGG:Nd-Ce-Cr ceramic is around 688 min, which is comparable with but slightly shorter than that of the

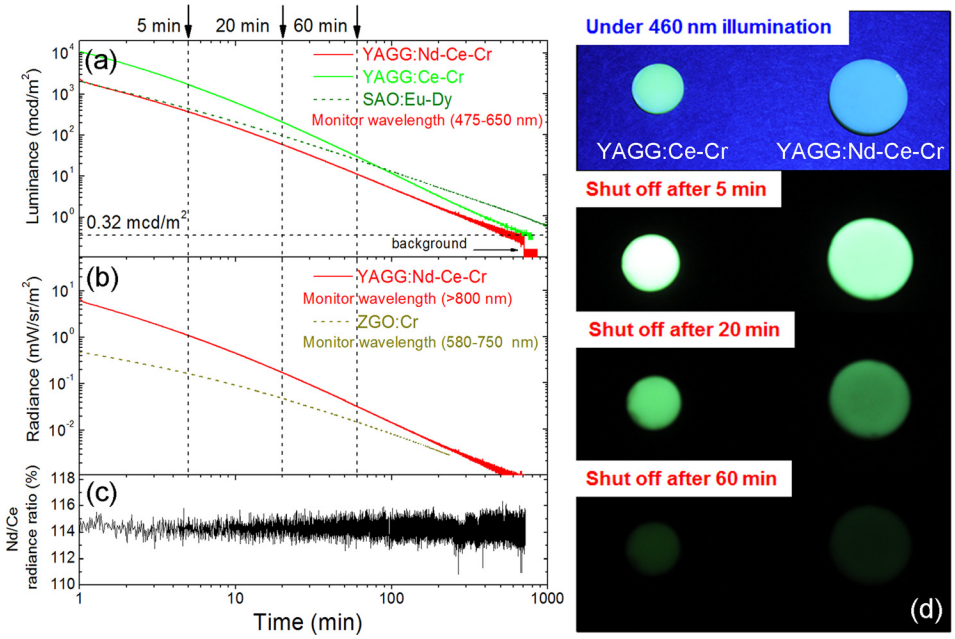

FIG. 2. Persistent decay curves of the YAGG:Nd-Ce-Cr ceramic: (a) luminance monitoring Ce^{3+} (YAGG:Ce-Cr and $SrAl_2O_4:Eu^{2+}$-Dy^{3+} ceramics as references), (b) radiance monitoring Nd^{3+} ($ZnGa_2O_4:Cr^{3+}$ ceramic as a reference), (c) Nd^{3+}/Ce^{3+} radiance ratio (%) against the monitoring time of the decay curve, and (d) photographs of the YAGG:Ce-Cr and YAGG:Nd-Ce-Cr ceramics under and after blue LED lamp (460 nm, 3 W output) illumination.

YAGG:Ce-Cr (about 808 min) ceramic, due to quenching of visible Ce^{3+} emission by the ET to Nd^{3+}.[25] Note that the luminance value 0.32 mcd/m^2 is the minimum value commonly used by the safety signage industry (about 100 times the sensitivity of the dark-adapted eye).[2] Because of this long green persistent luminescence at wavelengths very sensitive to the human's photopic vision, the YAGG:Nd-Ce-Cr nano-sized phosphor synthesized by nano-technical methods can act as a fluorescence marker convenient for surgeons to roughly confirm or even trace the marked tissues directly by human eyes without any electronic detectors in the difficult conditions typical of surgery dissection.

The persistent luminescent decay curve monitoring Nd^{3+} emission (>800 nm) of the YAGG:Nd-Ce-Cr sample after ceasing the same illumination is shown in Fig. 2(b), in which the decay curve of the standard $ZnGa_2O_4:Cr^{3+}$ (ZGO:Cr) ceramic under the same experimental condition is also plotted as a reference.[10] The NIR radiance value of the tri-doped sample at 60 min after ceasing the blue excitation (0.33×10^{-1} mW/Sr/m^2) is over 2 times higher than that of the widely used red persistent phosphor, ZGO:Cr (0.15×10^{-1} mW/Sr/m^2), indicating that this phosphor exhibits superior persistent luminescence both in the visible (Ce^{3+} emission) and NIR (Nd^{3+} emission) ranges.

The decay profiles of the Ce^{3+} and Nd^{3+} are quite similar in Figs. 2(a) and 2(b). The persistent radiance ratio (Nd^{3+}/Ce^{3+}) is plotted against the monitoring time of the whole decay curve as shown in Fig. 2(c). The result clearly suggests that the ratio remains almost constant (around 112%–114%) with time, which supports that the persistent luminescence from both ions originates from common electron trapping and de-trapping processes, where the NIR persistent luminescence of Nd^{3+} is due to the persistent ET process from Ce^{3+} to Nd^{3+} in the garnet host.[25]

Fig. 3 shows the two-dimensional (2D) mappings of TL glow curves of the YAGG:Ce-Cr and YAGG:Nd-Ce-Cr samples in order to see what kind of emission contributes to the TL glow peak at different temperatures. From the contour plot of the YAGG:Ce-Cr sample in Fig. 3(a), it can be seen that at increased temperatures, the TL spectrum is simply composed of two emission bands from Ce^{3+} and Cr^{3+}. While in the YAGG:Nd-Ce-Cr sample (see Fig. 3(b)), the NIR emission of Nd^{3+} appears at the same time due to the persistent ET process, which agrees well with its PersL

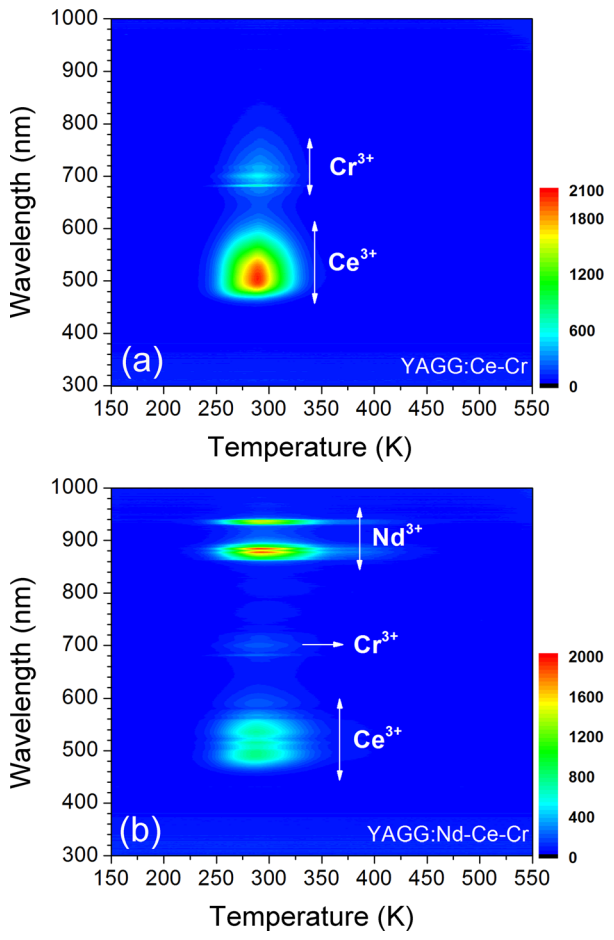

FIG. 3. Wavelength-temperature (λ-T) contour plots of the (a) YAGG:Ce-Cr and (b) YAGG:Nd-Ce-Cr ceramics.

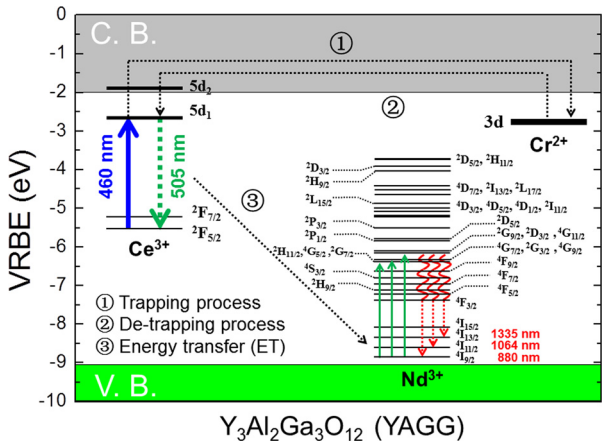

FIG. 4. The VRBE diagram for Ce^{3+}, Nd^{3+}, and Cr^{2+} energy levels in $Y_3Al_2Ga_3O_{12}$ (YAGG) host.

spectrum in Fig. 1(b). The intense TL glow peaks of both YAGG:Ce-Cr and YAGG:Nd-Ce-Cr samples lie in almost the same temperature range (around 295 K), close to RT and body temperature of Mammalia (around 36 °C). Since the TL peak temperature is correlated to the energy gap between the bottom of conduction band (CB) and the electron trap,[31] the identical glow temperature of the two samples indicates the same trapping and de-trapping processes in both,[22] where Cr^{3+} works as an efficient electron trap with ideal trap depth for long persistent luminescence in the host composition of $Y_3Al_2Ga_3O_{12}$.

The persistent luminescence mechanism of the YAGG:Nd-Ce-Cr phosphor is briefly explained by constructing the vacuum referred binding energy (VRBE) diagram[23,32,33] composed of Ce^{3+}, Nd^{3+}, Cr^{2+}, CB, and valence band energy levels in the $Y_3Al_2Ga_3O_{12}$ host (see Fig. 4). When the YAGG:Nd-Ce-Cr sample is charged by blue light, Ce^{3+} is promoted from the ground state ($^2F_{5/2}$) to the excited state of the lowest 5d energy level ($5d_1$), and the excited electron can "jump" into CB with thermal activation and then be trapped by the electron trapping center (Cr^{3+}).[22,23] At that time, Ce^{3+} is photo-oxidized into Ce^{4+} or ($Ce^{3+}+h^+$) and Cr^{3+} is formed to be Cr^{2+} or ($Cr^{3+}+e^-$) after capturing an electron (process ①).

Then the de-trapping process takes place with thermal release of the captured electron from the Cr^{2+} ($Cr^{3+}+e^-$) trap, and finally the excited state of the Ce ion, $(Ce^{3+})^*$ appears after capturing the released electron in the recombination process (process ②). The radiative relaxation gives a broad band emission of Ce^{3+}: $5d_1 \rightarrow {}^2F_{5/2}$, $^2F_{7/2}$, and the resonant ET occurs at the same time to Nd^{3+} ion (process ③), which is followed by rapid multi-phonon relaxation down to the $^4F_{3/2}$ excited level, and then finally induces the sharp luminescence bands of Nd^{3+}: $^4F_{3/2} \rightarrow {}^4I_{9/2}$, $^4I_{11/2}$, and $^4I_{13/2}$.

In summary, we developed a persistent phosphor ($Y_3Al_2Ga_3O_{12}$:Nd^{3+}, Ce^{3+}, Cr^{3+}) with multi-wavelengths (green light to NIR) and long (>10 h) persistent luminescence, which can be effectively excited by blue light illumination. The persistent radiance of the YAGG:Nd-Ce-Cr phosphor is over 2 times higher in the NIR region than that of the widely used $ZnGa_2O_4$:Cr^{3+} red persistent phosphor at 60 min after ceasing the excitation due to an efficient persistent energy transfer from Ce^{3+} to Nd^{3+}. Since its NIR persistent luminescence bands match well with the NIR-I and NIR-II bio-imaging windows, multi-functional applications not only in the *in vivo* bio-imaging but also in the drug delivery and cancerous chemotherapy can be expected in the near future by using this material as a nano-sized bio-probe with surface modification connected with functional organic radical groups.

We would like to acknowledge Professor Bruno. Viana who stayed at Kyoto University as a visiting professor for fruitful discussion on persistent phosphors and bio-imaging.

[1]S. K. Singh, RSC Adv. **4**, 58674 (2014).
[2]K. Van Den Eeckhout, D. Poelman, and P. F. Smet, Materials **6**, 2789 (2013).
[3]Q. le Masne de Chermont, C. Chanéac, J. Seguin, F. Pellé, S. Maîtrejean, J.-P. Jolivet, D. Gourier, M. Bessodes, and D. Scherman, Proc. Natl. Acad. Sci. U.S.A. **104**, 9266 (2007).
[4]T. Maldiney, A. Bessière, J. Seguin, E. Teston, S. K. Sharma, B. Viana, A. J. J. Bos, P. Dorenbos, M. Bessodes, D. Gourier, D. Scherman, and C. Richard, Nat. Mater. **13**, 418 (2014).
[5]Z. Pan, Y.-Y. Lu, and F. Liu, Nat. Mater. **11**, 58 (2012).
[6]T. Maldiney, C. Richard, J. Seguin, N. Wattier, M. Bessodes, and D. Scherman, ACS Nano **5**, 854 (2011).
[7]T. Maldiney, A. Lecointre, B. Viana, A. Bessière, M. Bessodes, D. Gourier, C. Richard, and D. Scherman, J. Am. Chem. Soc. **133**, 11810 (2011).
[8]F. Liu, W. Yan, Y.-J. Chuang, Z. Zhen, J. Xie, and Z. Pan, Sci. Rep. **3**, 1554 (2013).
[9]A. Bessière, S. Jacquart, K. Priolkar, A. Lecointre, B. Viana, and D. Gourier, Opt. Express **19**, 10131 (2011).
[10]Y. Zhuang, J. Ueda, and S. Tanabe, Appl. Phys. Express **6**, 052602 (2013).
[11]Y. Zhuang, J. Ueda, and S. Tanabe, J. Mater. Chem. C **1**, 7849 (2013).
[12]Y. Zhuang, J. Ueda, S. Tanabe, and P. Dorenbos, J. Mater. Chem. C **2**, 5502 (2014).
[13]J. Xu, J. Ueda, and S. Tanabe, Opt. Mater. Express **5**, 963 (2015).
[14]J. Xu, J. Ueda, Y. Zhuang, B. Viana, and S. Tanabe, Appl. Phys. Express **8**, 042602 (2015).
[15]A. M. Smith, M. Mancini, and S. Nie, Nat. Nanotechnol. **4**, 710 (2009).
[16]X. Peng, N. Komatsu, S. Bhattacharya, T. Shimawaki, S. Aonuma, T. Kimura, and A. Osuka, Nat. Nanotechnol. **2**, 361 (2007).
[17]M. Bruchez, M. Moronne, P. Gin, S. Weiss, and A. P. Alivisatos, Science **281**, 2013 (1998).
[18]J. Ueda, T. Shinoda, and S. Tanabe, Opt. Mater. Express **3**, 787 (2013).
[19]N. Yu, F. Liu, X. Li, and Z. Pan, Appl. Phys. Lett. **95**, 231110 (2009).
[20]Y. Teng, J. Zhou, Z. Ma, M. M. Smedskjaer, and J. Qiu, J. Electrochem. Soc. **158**, K17 (2011).
[21]J. Ueda, S. Tanabe, and T. Nakanishi, J. Appl. Phys. **110**, 053102 (2011).
[22]J. Ueda, K. Kuroishi, and S. Tanabe, Appl. Phys. Lett. **104**, 101904 (2014).
[23]J. Ueda, P. Dorenbos, A. J. J. Bos, K. Kuroishi, and S. Tanabe, J. Mater. Chem. C **3**, 5642 (2015).
[24]J. Xu, J. Ueda, K. Kuroishi, and S. Tanabe, Scr. Mater. **102**, 47 (2015).
[25]S. Möller, A. Hoffmann, D. Knaut, J. Flottmann, and T. Jüstel, J. Lumin. **158**, 365 (2015).
[26]M. Yamaga, Y. Oda, H. Uno, K. Hasegawa, H. Ito, and S. Mizuno, J. Appl. Phys. **112**, 063508 (2012).
[27]J. X. Meng, J. Q. Li, Z. P. Shi, and K. W. Cheah, Appl. Phys. Lett. **93**, 221908 (2008).
[28]D. Jia, R. S. Meltzer, W. M. Yen, W. Jia, and X. J. Wang, Appl. Phys. Lett. **80**, 1535 (2002).
[29]D. Jia, X. J. Wang, W. Jia, and W. M. Yen, J. Appl. Phys. **93**, 148 (2003).
[30]R. Zhong, J. Zhang, X. Zhang, S. Lu, and X. J. Wang, Appl. Phys. Lett. **88**, 201916 (2006).
[31]K. Van den Eeckhout, P. F. Smet, and D. Poelman, Materials **3**, 2536 (2010).
[32]P. Dorenbos, J. Electrochem. Soc. **152**, H107 (2005).
[33]P. Dorenbos, J. Lumin. **134**, 310 (2013).